

# ADVANCED OPTICAL MATERIALS

## Supporting Information

for *Adv. Optical Mater.*, DOI: 10.1002/adom.202102835

### Thermal Runaway of Silicon-Based Laser Sails

*Gregory R. Holdman, Gabriel R. Jaffe, Demeng Feng,  
Min Seok Jang, Mikhail A. Kats,\* and Victor W. Brar*

# Supporting Information

## Thermal runaway of silicon-based solar sails

Gregory R. Holdman\* and Gabriel R. Jaffe,<sup>1,\*</sup> Min Seok Jang,<sup>2</sup>  
Demeng Feng and Mikhail A. Kats,<sup>3</sup> and Victor Watson Brar<sup>†,1</sup>

<sup>1</sup>*Department of Physics, University of Wisconsin-Madison, Madison WI 53706 USA*

<sup>2</sup>*School of Electrical Engineering, Korea Advanced Institute of Science and Technology, Daejeon 34141, Korea*

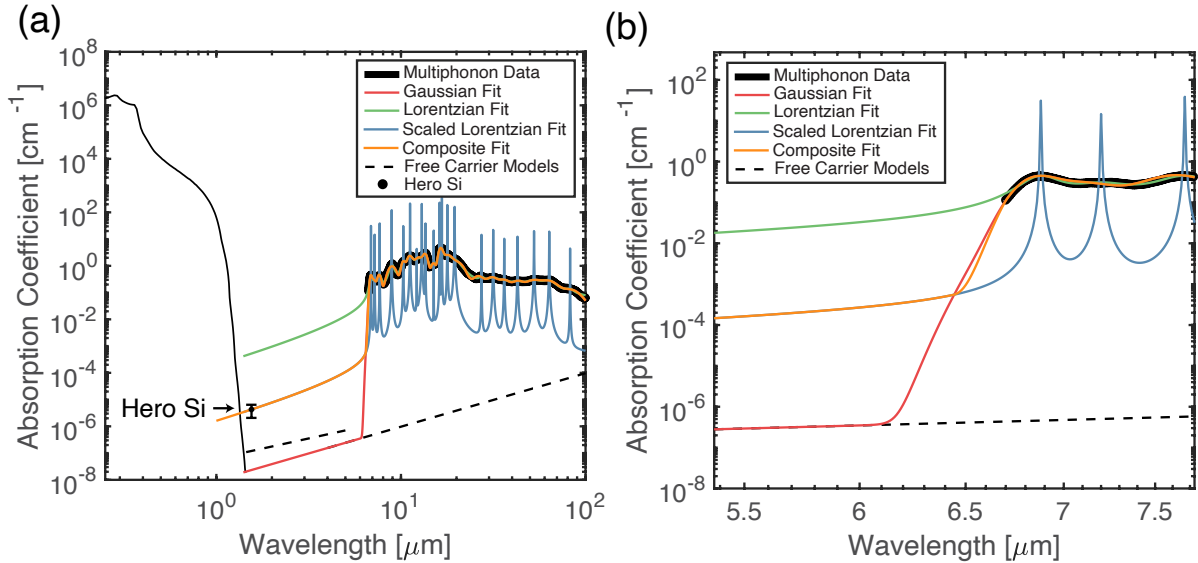
<sup>3</sup>*Department of Electrical and Computer Engineering,  
University of Wisconsin-Madison, Madison WI 53706 USA*

\*The authors contribute equally to this paper.

†Email: vbrar@wisc.edu

### I. MODELING OF THE SI ABSORPTION COEFFICIENT

The composite absorption model for Si presented in Fig. 2 of the main text includes two different models of the free carrier absorption coefficient,  $\alpha_{FC}$ . The model from Ref. [1] is used for wavelengths of 1.45–4  $\mu\text{m}$ , the model from Ref. [2] is used from 5–100  $\mu\text{m}$ . Because both models appear to be equally good and we expect the wavelength dependence of the free-carrier absorption to be a smooth function, we perform a linear interpolation between the two models from 4–5  $\mu\text{m}$  in order to avoid an unphysical discontinuity. These models are shown in Fig. S1 without the interpolation as dashed black lines. The thin solid black line denotes the absorption below 1.45  $\mu\text{m}$  from Ref. [3] and the thick black line is the multi-phonon absorption data from Ref. [4, 5]. To our knowledge, the lowest demonstrated absorption of Si at 1.55  $\mu\text{m}$  is  $4.28 \times 10^{-6} \text{ cm}^{-1}$  and is denoted in Fig. S1 as a solid black circle and labeled as ‘Hero Si’.[6] The absorption of Si from 7–100  $\mu\text{m}$ , which at room temperature is dominated by multi-phonon absorption, has been measured; however, the tail from these absorption bands at wavelengths shorter than 7  $\mu\text{m}$  has not.[4, 5]



\*

Figure S1. (a) The absorption of Si as a function of wavelength. Literature data and models of the absorption are shown as black lines and circles.[1–6]. Fits to the multi-phonon data assuming either Lorentzian or Gaussian peaks are shown in green and red, respectively. Note, the orange, green and red curves overlap at wavelengths  $>7\mu\text{m}$ . Scaling the Lorentzian fit peak widths such that the tail passes through the Hero Si data point at  $1.55\mu\text{m}$  produces the blue curve. The composite model used in the calculations in the main text consists of the scaled Lorentzian fit at short wavelengths and the Gaussian fit at long wavelengths and is shown in orange. The orange and blue curves overlap below  $6.43\mu\text{m}$ . (b) The absorption data and fits pictured in (a) over a narrower wavelength range. The composite fit (orange) linearly interpolates between the scaled Lorentzian fit (blue) and Gaussian fit (red) from  $6.43\text{--}6.70\mu\text{m}$ .

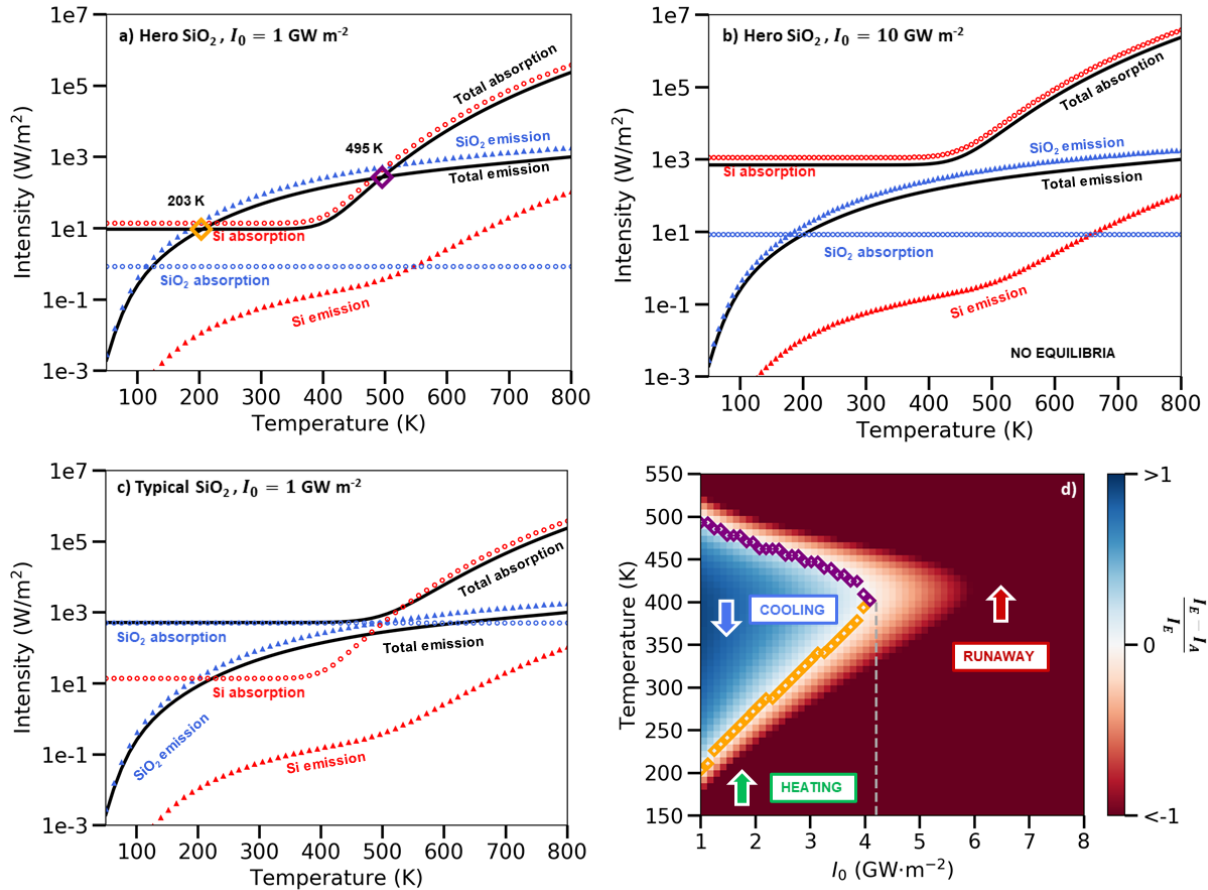


Figure S2. Replication of Fig. 3 in the main text, but for a Si/SiO<sub>2</sub> heterostructure with a solid layer of 450 nm Si on 200 nm SiO<sub>2</sub>. (a–c) Absorbed and thermally emitted intensities versus temperature for the Si/SiO<sub>2</sub> heterostructure made from either Hero or Typical SiO<sub>2</sub> and illuminated with an incident laser intensity  $I_0$ . Stable (orange) and unstable (purple) equilibrium temperatures are labeled as diamonds. Note, there is no equilibrium temperature for Typical SiO<sub>2</sub> at  $I_0 = 1\text{ GW}\cdot\text{m}^{-2}$  or Hero SiO<sub>2</sub> at  $I_0 = 10\text{ GW}\cdot\text{m}^{-2}$ . Absorbed and emitted intensities for the complete laser sail are shown in black while the contribution of the Si and SiO<sub>2</sub> layers are shown in red and blue, respectively. Dotted lines are used to indicate the Si absorption and SiO<sub>2</sub> emission because they overlap with the total absorption and emission. (d) Normalized difference in emissive intensity and absorptive intensity as a function of temperature  $T$  and incident intensity  $I_0$  for a sail made with Hero SiO<sub>2</sub>. Stable and unstable equilibrium temperatures are indicated as orange and purple diamonds, respectively. The blue and green arrows indicate the zones where the sail will either cool or heat to a stable equilibrium temperature below  $I_0 \approx 4.1\text{ GW}\cdot\text{m}^{-2}$ . Otherwise, thermal runaway occurs.

We fit the multiphonon absorption peaks with Lorentzian lineshapes in order to extrapolate between the short-wavelength edge of the multiphonon data at  $7\mu\text{m}$  and the measured absorption at  $1.55\mu\text{m}$ . First, the absorption contribution from free carriers is subtracted from multiphonon resonances. A least-squares fit is performed using Lorentzians centered at each of the allowed two- and three-phonon absorption peaks, and the carbon impurity peak.[5, 7] Additional absorption peaks at 20, 27, 32, 36, 43, 53, 64, and  $82\mu\text{m}$  were included in the fit to better match the absorption features seen in the data at long wavelengths. We note that these energies are too small to arise from multiphonon absorption processes and that the multi-phonon and carbon impurity peaks are the dominant contributors to the absorption tail at  $1.55\mu\text{m}$ . The tail of the best fit Lorentzian model (green curve in Fig. S1) predicts absorption

several orders of magnitude above the measured Hero Si absorption. This indicates that the width of the peaks in the multiphonon data is the result of inhomogeneous broadening. The broadened Lorentzian peaks will appear Gaussian near the center of each peak. A fit using Gaussian lineshapes instead of Lorentzians (red curve) matches the data well near the peaks but decays too rapidly at short wavelengths to capture the expected long tail behavior of Lorentzians. We therefore scale the widths of the peaks in the best fit Lorentzian model until the tail passes through the Hero Si absorption data point at  $1.55 \mu\text{m}$  (blue curve). The model for the multi-phonon absorption coefficient,  $\alpha_L(\lambda)$ , as a function of wavelength,  $\lambda$ , used in the main text consists of the scaled Lorentzian fit for  $\lambda < 6.43 \mu\text{m}$ , the best fit Gaussian model for  $\lambda > 6.70 \mu\text{m}$ , and then a linear interpolation between the two fits from  $6.43\text{--}6.70 \mu\text{m}$ . This composite fit is shown in orange in Fig. S1.

## II. COMPARISON OF THE EMISSION AND ABSORPTION OF THE METASURFACE TO A CONTINUOUS SLAB

In the main text, we showed that a particular highly reflective metasurface will experience thermal runaway at all incident intensities  $I_0 > 4.8 \text{GW}\cdot\text{m}^{-2}$ . In this section, we perform the same analysis on a heterostructure of 450 nm of Si on 200 nm of SiO<sub>2</sub>. The layer thicknesses of this heterostructure are identical to those of the the metasurface we analyzed in the main text; however, the Si layer in the heterostructure is a continuous slab instead of individual blocks. We find that the heterostructure geometry also exhibits the thermal runaway behavior of the metasurface, and has an even lower maximum  $I_0$ , above which no equilibrium temperature exists.

The emission intensity  $I_E$  is calculated in the same way as described in the main text while absorption  $I_A$  is now calculated analytically, since the surface is translationally invariant. We plot the results in Fig. S2. We see that for the high-quality Hero SiO<sub>2</sub> and  $I_0 = 1 \text{GW}\cdot\text{m}^{-2}$ , the stable temperature has risen to 203 K from the 177 K of the metasurface, while the unstable temperature has lowered to 495 K from 516 K. In Fig. S2d, we see this also has the effect of lowering the incident intensity limit to  $I_0 = 4.1 \text{GW}\cdot\text{m}^{-2}$ . The heterostructure is less thermally robust than the metasurface because the total absorption in the Si has risen slightly from the increased surface coverage.

The AD of the heterostructure sail design suffers for two reasons. First, as seen in Fig. S2d, the maximum  $I_0$  the heterostructure can withstand is lower than that of the metasurface in the main text. Second, it is far from being highly reflective across the Doppler band of interest. Using the reflectivity spectrum and  $I_0 = 4.1 \text{GW}\cdot\text{m}^{-2}$ , we calculate the AD to be  $D = 532 \text{Gm}$ . This is more than 4 times larger than the 120 Gm AD of the metasurface in the main text.

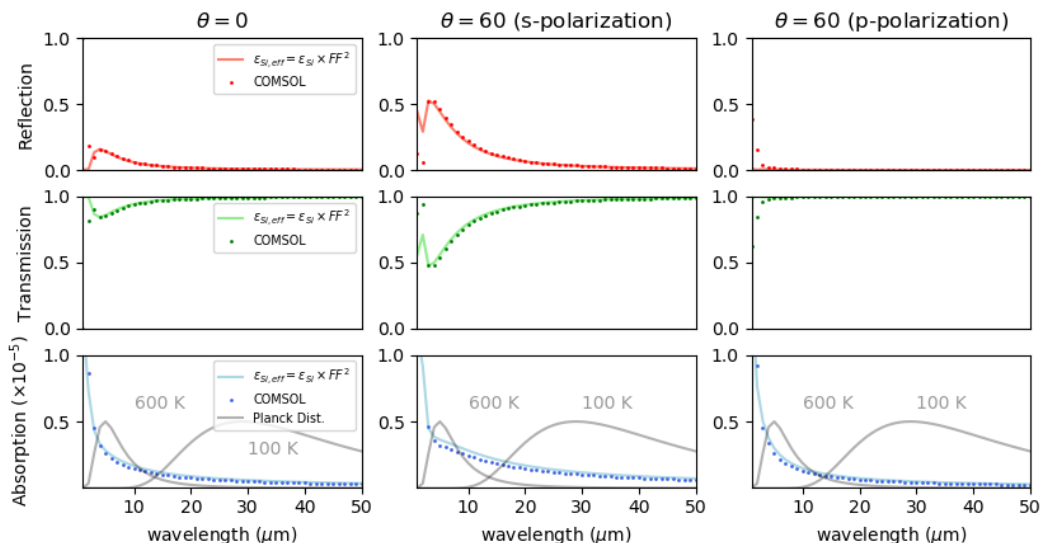


Figure S3. Comparison of the reflection, transmission, and absorption spectra of the metasurface using the analytic approximation (i.e. assuming Si to be a solid slab with an effective index) and full-wave simulations in COMSOL. For wavelengths longer than  $2 \mu\text{m}$ , the agreement is very good, implying that this approximation is valid for calculations of the metasurface's emissivity.

### III. EFFECTIVE MEDIUM APPROXIMATION IN MID-INFRARED AND BEYOND

The calculation of  $I_E(T) = I_E^s(T) + I_E^i(T)$ , requires performing an integration over all wavelengths, angles, and polarizations of interest using the formula

$$I_E^i(T) = \int_{\lambda_1}^{\lambda_2} d\lambda \int_0^{2\pi} d\phi \int_0^\pi d\theta \quad \epsilon_i(\lambda, \phi, \theta, T) \frac{hc^2}{\lambda^5} \frac{1}{\exp(hc/\lambda k_B T) - 1} \cos \theta \sin \theta, \quad (i = s, p). \quad (1)$$

The emissivity  $\epsilon_i(\lambda, \theta, \phi)$  ( $i = s, p$ ) varies as a function of  $\lambda$ ,  $\theta$ ,  $\phi$ , and  $i$ . To perform this calculation by sweeping the parameters in COMSOL would be extremely computationally intensive.

To simplify this calculation, we approximate the emissivity by replacing the blocks of Si with a slab of equal thickness 450 nm and refractive index  $n_{eff} = n_{Si} \times FF$  where  $FF = (430^2)/(670^2)$  is the filling factor. The geometry in this approximation is then a stack of two unpatterned slabs which has an analytical solution for the absorptivity  $\alpha_i(\lambda, \phi, \theta, T)$  using transfer matrices. Using Kirchoff's law of thermal radiation, we obtain  $\epsilon_i(\lambda, \phi, \theta, T) = \alpha_i(\lambda, \phi, \theta, T)$  analytically.

At mid-infrared to long-wave infrared wavelengths ( 2-100  $\mu\text{m}$  where thermal emission occurs), this approximation is valid. We have checked the validity of this approximation by comparing Python-based transfer matrix code with full-wave COMSOL simulations of the metasurface. We used indices  $n_{Si} = 11.7 + i10^{-5}$  and  $n_{SiO_2} = 2.1 + i10^{-5}$  for Si and SiO<sub>2</sub>, respectively. Simulations were performed at incident angles  $\theta = 0^\circ$  and  $60^\circ$ , polarizations  $s$  and  $p$ , and from  $\lambda = 1$  to 50  $\mu\text{m}$ . The reflection, transmission, and absorption were recorded as shown in Fig. S3. It is clear that the approximation aligns closely with the simulated result. Some deviation occurs below 2  $\mu\text{m}$  in wavelength, but this does not significantly affect the calculation of  $I_E(T)$  because the blackbody spectrum is quite weak at those wavelengths.

### IV. TRADE OFF IN SCALING OF STRUCTURE

As discussed in the main text, an important figure of merit for a light sail is its acceleration distance (AD).[8] This number is influenced not only by the maximum intensity the sail can survive, but also by the mass of the sail and the reflection spectrum over the Doppler band (1550 nm to 1900 nm). Prior to our analysis demonstrating the existence of a maximum survivable intensity, the metasurface geometry presented in the main text was chosen to maximize its reflectivity at 1550 nm. Here we optimize for the shortest possible acceleration distance by scaling the original structure and calculating how the reflectivity, mass, and maximum survivable intensity vary with structure geometry.

The scaling is shown in Figure S4a. All dimensions of interest are scaled by a factor  $x$  where  $x = 1$  is the original structure shown in the main text. The electric field changes with the structure as seen in Figure 4b. At  $x = 1.05$  ( $x = 0.95$ ) the magnitude of the field increases (decreases). In Figure S4c, we can see that this is caused by a shift in the spectral position of the resonance near 1300 nm. Scaling up shifts the resonance toward the driving laser wavelength of 1550 nm increasing the absorption. Simultaneously, the reflection plateau shifts into the Doppler band providing higher reflection. While the increased reflection ought to decrease the AD, the increased absorption will decrease the maximum intensity raising the AD. At some value of  $x$  is a minimum AD.

In Figure S4d, we show the impact of scaling the structure on both  $I_{Max}$  and the AD. As expected,  $I_{Max}$  decreases due to the increased absorption. Changes in the mass due to scaling are also accounted for, but not plotted here. The AD exhibits a minimum at  $x = 1.05$ , showing that the structure presented in the main text was close to optimal. The AD reduces from 148.9 Gm to 126.5 Gm when scaling the structure to be 5% larger, corresponding to a period of 703.5 nm, Si block height and width of 472.5 nm and 451.5 nm, and SiO<sub>2</sub> thickness of 210 nm. This demonstrates that the structure shown in the paper can not be improved much without performing an optimization in a much larger parameter space. Such work, however, is beyond the scope of this paper.

### V. PERFECT BLACKBODY EMISSION

Thermal runaway will still occur, even in the ideal case where the sail is able to thermally radiate as a perfect blackbody. While SiO<sub>2</sub> exhibits strong emission in the mid-infrared, the thickness of the SiO<sub>2</sub> layer in the geometry we consider in the main text is too thin to provide perfect blackbody emission. Layer thicknesses on the order of the wavelength of emission ( $\sim 10 \mu\text{m}$ ) would be needed to achieve anything close to perfect blackbody emission. As an example, if we assume a 10  $\mu\text{m}$  thick film with an absorption coefficient of  $10^3 \text{ cm}^{-1}$ , this yields a total emission of  $I_{BB}/e$  where  $I_{BB}$  is the blackbody emission. This is about 50 times thicker (and therefore 50 times heavier) than the SiO<sub>2</sub> in the design reported in the main text.

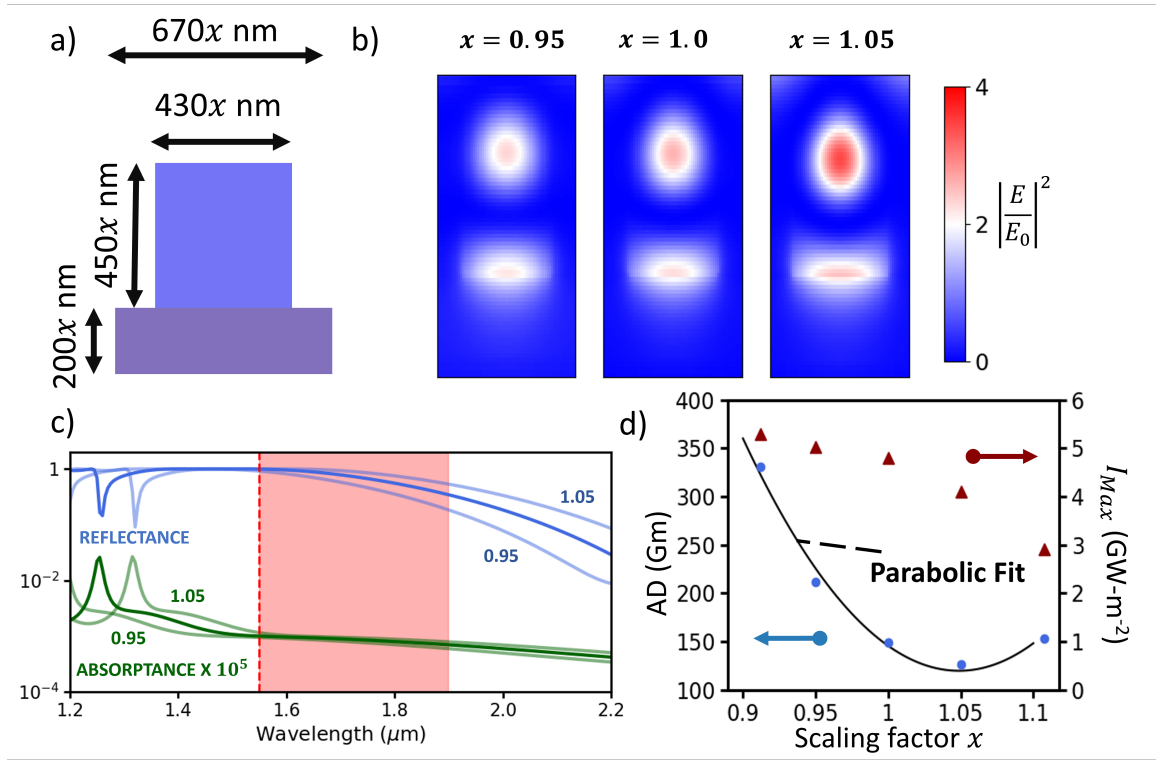


Figure S4. a) Schematic of the scaling of our metasurface. The scale factor  $x$  applies to all dimensions, including the out-of-plane width of the Si block ( $430x$ ) and period ( $670x$ ). b) Squared electric field magnitude at 1550 nm of the metasurface at different scaling factors. Field magnitude increases at higher scaling factors. c) Reflection and absorption spectra of the metasurface at different scaling factors. Absorption coefficient of silicon is chosen to correspond to  $I_0 = 1 \text{ GW}\cdot\text{m}^{-2}$  and  $T = 300 \text{ K}$ . Scaling the structure simply shifts the spectrum. d) AD versus scaling of the metasurface in the main text of the paper. Scaling the surface to by 5% larger results in an optimal AD of 126.5 Gm.

Figure S5 shows the thermal stability analysis assuming the  $\text{SiO}_2$  in the metasurface emits as a perfect blackbody (grey line). Performance does improve; the stable equilibrium temperature lowers to about 100 K and the unstable equilibrium temperature rises to 650 K. Furthermore, Figure S5b shows that the maximum survivable intensity  $I_{Max}$  rises to  $18.8 \text{ GW}\cdot\text{m}^{-2}$ . These gains in thermal stability and maximum survivable incident intensity would be offset by the significant increase in sail mass need to achieve such a large emissivity.

- [1] H. Rogne, P. J. Timans, and H. Ahmed, Infrared Absorption in Silicon at Elevated Temperatures, *Applied Physics Letters* **69**, 2190 (1996), <https://doi.org/10.1063/1.117161>.
- [2] D. K. Schroder, R. N. Thomas, and J. C. Swartz, Free Carrier Absorption in Silicon, *IEEE Journal of Solid-State Circuits* **13**, 180 (1978).
- [3] M. A. Green, Self-Consistent Optical Parameters of Intrinsic Silicon at 300K Including Temperature Coefficients, *Solar Energy Materials and Solar Cells* **92**, 1305 (2008).
- [4] F. A. Johnson, Lattice absorption bands in silicon, *Proceedings of the Physical Society* **73**, 265–272 (1959).
- [5] E. J. Wollack, G. Cataldo, K. H. Miller, and M. A. Quijada, Infrared properties of high-purity silicon, *Optics Letters* **45**, 4935 (2020).
- [6] J. Degallaix, R. Flaminio, D. Forest, M. Granata, C. Michel, L. Pinard, T. Bertrand, and G. Cagnoli, Bulk optical absorption of high resistivity silicon at 1550 nm, *Opt. Lett.* **38**, 2047 (2013).
- [7] M. Pradhan, R. Garg, and M. Arora, Multiphonon infrared absorption in silicon, *Infrared Physics* **27**, 25 (1987).
- [8] W. Jin, W. Li, M. Orenstein, and S. Fan, Inverse design of lightweight broadband reflector for relativistic lightsail propulsion, *ACS Photonics* **7**, 2350–2355 (2020).

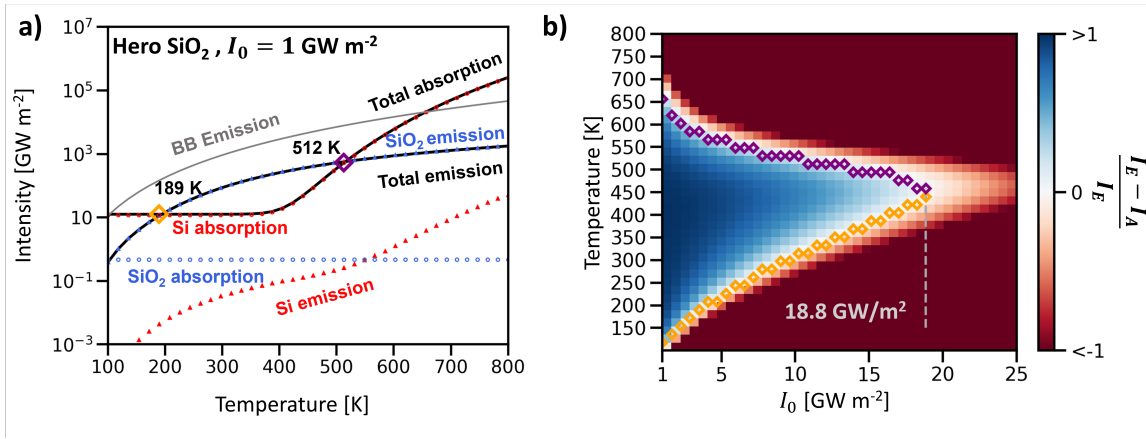


Figure S5. Thermal stability analysis for theoretical metasurface using Hero SiO<sub>2</sub> for absorption, but assuming perfect blackbody emission for radiative cooling. (a) calculation of the thermal runaway temperature (650 K) and equilibrium temperature (100 K) for a perfect blackbody emitter. (b) Calculated regions of thermal runaway heating (red) and equilibrium cooling (blue) for the metasurface, indicating a maximum laser intensity of 18.8 GW m<sup>-2</sup>. Purple and orange dots represent thermal runaway and equilibrium temperatures, respectively.